Journal of Advanced Engineering Trends
ISSN : 2682 - 2091

Vol.43, No.1. January 2024

http://jaet.journals.ekb.eg

Parametric analysis on the performance of a hybrid absorption desalination-cooling system

El-Sadek. H. NourEldeen[1*], K. Harby[1,2]

[1] *Assoc. Prof., Mech. Power Engineering and Energy Department, Faculty of Engineering, Minia University, 61519, Minia, Egypt*

[2] *Assoc. Prof., Mech. Engineering Department, College of Engineering, Taibah University, Al-Madinah Al-Munawarah, Saudi Arabia*

A R T I C L E I N F O

Article history:
Received:
Accepted:
Online:

Keywords:
Hybrid
Absorption
Desalination
Cooling
Energy efficiency

A B S T R A C T

The demand for new technologies due to the global energy shortage, water scarcity, and environmental issues have been a scientific worry and challenge all over the world nowadays. Conventional desalination and cooling systems consume a large amount of energy and harm the environment. In the actual study, performance of a proposed hybrid absorption-desalination cooling system (ABDCS) is investigated theoretically. The main advantage of this system is the ability to utilize effectively low-grade heat source to produce simultaneously both desalinated water and cooling effect. A mathematical MATLAB code is developed and validated to simulate the performance of the system. Results showed that, the maximum system COP is obtained at 85 ^oC driving heat source temperature. This makes the proposed system suitable for low-grade heat sources and heat recovery process, which can be easily obtained from low grade heat source. At this temperature, the obtained cooling effect is 346 kW, the coefficient of performance (COP) is 0.774, and 13.88 m^3day^{-1} desalinated water production. Increasing heat source temperatures and cooling water temperatures increasing the STEC linearly from 754 to 806 kWh/m^3 and from 722 to 812 kWh/m^3 respectively along the range of temperatures tested. On the other, the STEC decreased from 814 to 716 kWh/m^3 with increasing in the chilled water.

1. Introduction

The rapidly increase in the rate of energy consumption for freshwater production and cooling demand forces many researchers to develop alternative solutions and propose innovative technologies. The availability of fresh-water and cooling are considered the main factors to accomplish sustainable development and improvement in the quality of life. The fast increase in the rate of energy consumption for freshwater production and cooling demand obliges the scientists to develop and improve alternative and innovative technologies. The availability of fresh-water and cooling are considered the major factors to accomplish sustainable development and improvement in the quality of life.

The main usual used cooling technologies nowadays is depending on the traditional vapor compression refrigeration cycle (VCRC), due to its high COP [1]. These cycles consume a large amount of high-grade energy which is mostly gained by burning fossil fuels and working with environmentally unfriendly refrigerants [2, 3]. In Middle East, air-conditioning cycles consume about 32% of the total energy systems are used mainly nowadays to meet the increasing demand of freshwater [4, 5]. Production of 1 million m3/day of fresh water requires 10 million tons of oil per year [6]. Most of the actual desalination cycles depend on traditional technologies. These systems are very energy intensive process because of high capital cost and energy consumption and produce great amounts of waste and pollute the environment [7, 8].

Revised:7 May , 2022, Accepted:18 June , 2022

Renewable energy sources and new combined and innovative technologies have acquired more attraction recently for both cooling and desalination systems due to their ability to save energy and minimize environmental impacts [9]. Solar energy considered the primarily used in desalination systems to produce fresh water and supply the required comfort conditions. The large increases in cooling and potable water demands occur in locations where solar energy is abundant. Different types of solar cooling and water desalination systems have been utilized recently for individual cooling and water desalination applications [10]. Coupling both cooling and desalination in one technology appears to be attractive not only to minimize the rate of energy consumption and provide more flexible operation but also for environmental issues. The dual effect produced by this process, allows the cycle to fully employ all the thermal energy available.

The conventional absorption cooling system has the characteristic of being able to operate by low temperature range and considered environmentally friendly system. The main differences between mechanical vapour compression system and absorption system are the method of transferring the working fluid from the lower pressure system to the higher-pressure system and the working fluid used.

Different research have been done on performance of absorption cooling systems [11, 12]. Rosiek [13] investigated experimentally the exergy and performance analysis of a solar-powered 70 kW single effect LiBr-H2O absorption cooling

system with a traditional flat-plate solar collector in Spain. The results demonstrated that, the maximum performance (COP) obtained from the proposed system was 0.6 at hot water temperatures ranges between 70 to 80°C. Furthermore, Bellos et al. [14] presented exergetic, energetic, and economic investigations of a solar-powered absorption cooling system. Four collector types are used in the study including flat plate, evacuated tube, compound parabolic, and parabolic trough collector. The results showed that the maximum solar COP and solar exergetic efficiency is obtained with the system attached with the parabolic trough collector because of their high thermal efficiency compared with the other collector used. Li et al. [15] studied the performance of 23-kW solar powered single-effect LiBr-H2O absorption refrigeration system using 56 m2 parabolic trough collector. The experiment results showed that the maximum daily COP was varied between 0.11 and 0.27 in the sunny days. Cascales et al. [16], investigated the performance of solar driven single effect absorption cooling system working with LiBr-H2O theoretically. The system was built for air-conditioning of a classroom in an educational center in Puerto Lumbreras, Murcia, Spain. Different mathematical models have been developed to simulate and predict the system performance. Tsilingiris [17] developed a theoretical model for a solar cooling system for domestic applications in homes and evaluated the economic performance of the cooling system at the cost of fossil fuels. Mazloumi et al. [18] investigated the thermal performances of a single effect LiBr–H2O absorption cooling system powered by parabolic trough solar collector. The results showed that the optimal capacity of the used storage tank significantly affects system performance. Yeung and al., [19] investigated experimentally the performance of solar driven 4.7 kW absorption cooling system at the University of Hong Kong. Flat plate solar collectors with a total area of 38.2 m² with water storage tank are used. Results demonstrated that the collector efficiency was 37.5%, the system efficiency 7.8% and solar fraction of 55%, respectively.

Searching for new and innovative technology and configuration are of the most important subject nowadays for desalination and cooling systems to enhance the energy efficiency and protect the environment. In this research, parametric analysis on the performance of a proposed solar powered hybrid absorption desalination-cooling system (ABDCS) is presented and investigated theoretically. This is a promising study which has not been investigated yet. Operation of this cycle is like the traditional solar powered absorption cooling system (ABS). However, in the proposed ABDCS a simultaneously fresh water and cooling effect are produced. In the proposed ABDCS the expansion valve between the condenser and evaporator does not exist. The condensed water vapor from the condenser is used as the produced desalinated water and the evaporator is feed with the feed sea water. Mathematical model is developed and validated to simulate the performance of the ABDCS and investigate the effect of different operating parameters.

2. System description

The system is consisting of two main subsystems namely, solar heating subsystem and the proposed hybrid absorption desalination-cooling system (ABDCS). A schematic diagram of the proposed hybrid absorption desalination-cooling system (ABDCS) is showed in Figure 1. The basic ABDCS processes is schematically shown in Dühring diagram in Figure 2.

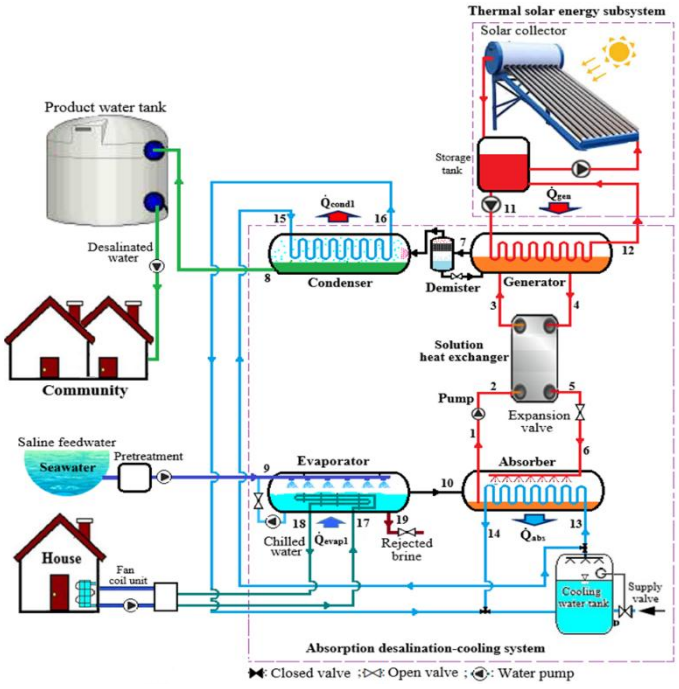

Figure 1: Schematic diagram of the proposed ABDCS

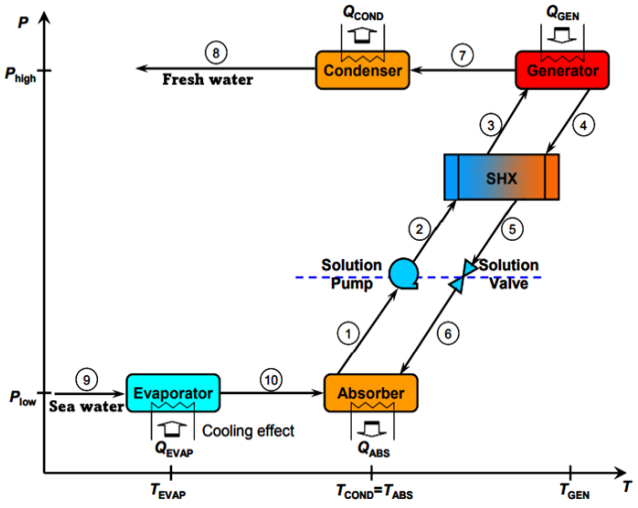

Figure 2: Schematic diagram of proposed ABDCS in Dühring diagram

The proposed ABDCS composed of four main components, namely absorber, desorber (generator), condenser, and evaporator. In addition, the system contains working fluid which consists of refrigerant and absorbent. Other supporting components required

for the system are solution pump, solution valve, refrigerant valve, and solution heat exchanger (SHX). In the cycle, the refrigerant subjects a phase change in the condenser and evaporator, and the absorbent solution subjects a concentration change in the absorber and the generator. The evaporator is feed with the feed sea water and the condensed water vapor after the condenser is used as the produced fresh water.

Through the cycle, the feed seawater goes firstly via the pre-treatment process which prevents fouling and chemical solutions that can decrease the performance of the system. The treated seawater then passes into the evaporator and evaporates at low pressure by the heat extracted from the chilled water ($\dot{Q}_{evap}$) supplies cooling capacity for space cooling. The water vapor from the evaporator is then absorbed by the strong solution exist at the absorber. The relatively weak solution in the absorber (at point 1) is then pumped into the generator (at point 3) passes through the solution heat exchanger. The L_iB_r/H_2O solution is preheated by passing the strong solution during a heat exchanger.

The hot water in the generator is provided from the hot water tank of the heating source by thermal solar energy subsystem. The heat energy supplied to the generator (at point 11) heats the weak solution and causes to separate the water vapor from the L_iB_r (since L_iB_r is not volatile). The water vapor then passes to the condenser at line (7), while the strong solution returns to the absorber element at line (6) through the expansion valve unit after passing through the heat exchanger. A demister unit is also used after the generator to separate and stop any entrainment droplet of the LiBr to passes with the water vapor to the condenser (Altaee, 2012) [20] (as shown in Figure 1).

The condensed water is then collected as the produced freshwater at line 8. The freshwater is formed by condensation of the water vapor, which is collected after the condenser and passed to the product freshwater tank. At each stage, the product water is also flash boiled so that it can be cooled, and the surplus heat recovered for preheating the feedwater.

The heat of condensation and absorption is taken out by the cooling water resulted from a cooling tower as shown in Figure 1. The cooling water flows through the absorber firstly and then passes into the condenser because the absorber temperature affects the cycle efficiency more than the condensing temperature. The brine mb at the evaporating unit is gathered and discharged periodically from the evaporators into a brine storage at point 19.

3. Thermodynamic modeling

To evaluate the performance of the proposed ABDCS, a thermodynamic model based on the mass and energy balances of each element in the system shown in Fig. 2 is developed. Table 1 demonstrated the equation system for each element of the proposed ABDCS [10]. Table 2 shows the used design parameters. Some of assumptions are applied through analysis to simplify the model:

- No pressure drops through the elements, excluding the expansion valves.
- Heat losses, kinetic and potential energy effects are neglected.
- Saturated liquid conditions at outlets of absorber, condenser and generator and saturated vapor conditions at evaporator outlet.

Table1: Mass and energy balance equation for the proposed ABDCS (10)

Component	Mass balance	Energy balance
Generator	$\dot{m}_3 = \dot{m}_4 + \dot{m}_7$ (1) $\dot{m}_3 x_3 = \dot{m}_4 x_4$ (2)	$\dot{Q}_{gen} = \dot{m}_4 h_4 + \dot{m}_7 h_7 - \dot{m}_3 h_3$ (3) $\dot{Q}_{gen} = \dot{m}_{11}(h_{11} - h_{12})$ (4) $\dot{Q}_{gen} = UA_{gen}\Delta T_{Lm,gen}$ (5)
Condenser	$\dot{m}_7 = \dot{m}_8$ (6) $\dot{m}_8 = \dot{m}_{desalinate}$ (7)	$\dot{Q}_{con} = \dot{m}_7 h_7 - \dot{m}_8 h_8$ (8) $\dot{Q}_{con} = \dot{m}_{15}(h_{16} - h_{15})$ (9) $\dot{Q}_{con} = UA_{con}\Delta T_{Lm,con}$ (10)
Evaporator	$\dot{m}_9 = \dot{m}_{10} + \dot{m}_{19}$ (11) $\dot{m}_9 = \dot{m}_{b,ro}$ (12) $\dot{m}_{19} = \dot{m}_{b,ab}$ (13)	$\dot{Q}_{evap} = \dot{m}_{10} h_{10} + \dot{m}_{19} h_{19} - \dot{m}_9 h_9$ (14) $\dot{Q}_{evap} = \dot{m}_{17}(h_{18} - h_{17})$ (15) $\dot{Q}_{evap} = UA_{evap}\Delta T_{Lm,evap}$ (16)
Absorber	$\dot{m}_1 = \dot{m}_6 + \dot{m}_{10}$ (17) $\dot{m}_1 x_1 = \dot{m}_6 x_6 + \dot{m}_{10} x_{10}$ (18)	$\dot{Q}_{abs} = \dot{m}_6 h_6 + \dot{m}_{10} h_{10} - \dot{m}_1 h_1$ $\dot{Q}_{abs} = \dot{m}_{13}(h_{14} - h_{13})$ (19) $\dot{Q}_{abs} = UA_{abs}\Delta T_{Lm,abs}$ (20)
Heat exchanger	$\dot{m}_2 = \dot{m}_3$ (21) $\dot{m}_4 = \dot{m}_5$ (22)	$\dot{Q}_{hex,cold} = \dot{m}_1(h_3 - h_2)$ (23) $\dot{Q}_{hex,hot} = \dot{m}_4(h_4 - h_5)$ (24) $\varepsilon_{SHX} = (T_4 - T_5)/(T_4 - T_2)$ (25)
Expansion valve	$\dot{m}_5 = \dot{m}_6$ (26)	$h_5 = h_6$ (27)
Pump solution	$\dot{m}_1 = \dot{m}_2$ (28)	$\dot{W}_{pump} = h_2 - h_1$ (29) $\dot{W}_{pump} = \frac{\dot{m}_1 \upsilon_1 (P_{high} - P_{low})}{\eta_{pump}}$ (30)

Table 2: Design parameters of the proposed hybrid ABDCS

Input parameters	value
Heat exchanger effectiveness, ε_{SHX}	0.8
Pump mass flow rate, $\dot{m}_1$	1.0 kg/s
Overall heat transfer coefficient of the absorber, UA_{abs}	72.99 kW/K
Overall heat transfer coefficient of the condenser , UA_{cond}	157.1 kW/K
Overall heat transfer coefficient of the generator, UA_{gen}	20.71kW/K
Overall heat transfer coefficient of the evaporator, UA_{evap}	96.73kW/K

The demister used after the generator and generated pressure drop. To calculate the pressure, drop, correlation developed by by E1-Dessouky et ai. [21] is used.

$$\Delta p_{demister} = 9.583 \times 10^4 (\rho_p)^{1.597} (V)^{0.7107} (X_p)^{1.388} \quad (31)$$

where ρ_p is the demister pad density, X_p is the pad thickness, V is the vapor velocity through the pad.

The proposed ABDCS produces simultaneously both desalinated water and cooling effect. To investigate the overall performance of the system, total distillate water production ($\dot{Q}_{desalinate}$), cooling effect ($\dot{Q}_{cap}$), and specific electrical energy consumption (SEEC) are evaluated.

The desalinated mass flow rate of the proposed ABDCS is given by:

$$\dot{m}_{desalinate} = \dot{m}_8 \quad (32)$$

The distillate water production ($\dot{Q}_{desalinate}$) is given by:

$$\dot{Q}_{desalinate} = \dot{m}_{desalinate} \square f g_{(T_{cond})} \quad (33)$$

Where, h_{fg} is the water latent heat of vaporization measured in $kJkg^{-1}$.

The system cooling effect is given by:

$$\dot{Q}_{cap} = \dot{Q}_{evap} = (\dot{m} C_p)_{c \square w} (T_{c \square w,out-18} - T_{c \square w,in-17}) \quad (34)$$

The driving heat source ($\dot{Q}_{gen}$):

$$\dot{Q}_{gen} = (\dot{m} C_p)_{\square w} (T_{\square W,in-11} - T_{\square w,out-12}) \quad (35)$$

The system performance is given by:

$$COP = \frac{\dot{Q}_{evap}}{\dot{Q}_{gen} + \dot{W}_{pump}} \quad (36)$$

The specific thermal energy consumption (STEC) or the specific heat consumption is a measure of the amount of thermal energy needed to produce a unit (1 m^3/h) of distilled water output.

$$\text{STEC} = \frac{\dot{Q}_{gen} \times 24}{\dot{m}_{destillate}} \quad kWh/m^3 \quad (37)$$

where $\dot{Q}_{gen}$ is the required heat input from the generator (kW), $\dot{m}_{distelate}$ is flow rate of the product (m^3/day).

4. Result and discussion

Parametric analysis of the performance of the proposed hybrid absorption desalination-cooling system is investigated, validated, and evaluated under typical and various operating conditions in this section.

4.1 Model validation

As mentioned before, there are no past experimental or theoretical studies available for validating the proposed ABDCS are found in the open literature. Therefore, to verify the accuracy of the developed model of the proposed hybrid ABDCS, the simulation results can be validated by comparing them with the data available for conventional absorption cooling system (ABS). In this study, the developed model of proposed model is validated by the experimental results reported by Balghouthi et al. [24] for conventional single stage absorption cooling system (ABS) as shown in Table 3.

Table 3: Comparison between simulation results from Balghouthi et al. [24] and this study.

Parameter	Balghouthi et al. [24]	This study	Deviation (%)
$\dot{Q}_{abs}$, kW	14.67	14.72	0.33
$\dot{Q}_{cond}$, kW	11.89	11.84	-0.42
$\dot{Q}_{gen}$, kW	15.26	15.30	0.326
$\dot{Q}_{evap}$, kW	11.31	10.11	-11.87
COP, (-)	0.74	0.84	11.90
$\dot{m}_{salinate}$, m^3/day	-	0.51	-

It can be seen that, under at same operating and design conditions, the simulation results of the proposed model show good agreement with the published results from reference [24] for ABS. However, there are some of discrepancies between our results of ABDCS model and those of ABS model and are in quite acceptable range with a maximum deviation of about 11.90 %. These deviations are due to our system produce simultaneously desalinated water and cooling effect and the system of reference [24] produces only cooling effect. It is therefore concluded that the developed model is reliable and can be used to investigate the performance of the proposed hybrid ABDCS.

4.2 Parametric analysis of the proposed system

Figures 3 (a and b) present the effect of generator water temperature on the system performance COP and cooling capacity and on the rate of desalinated water ($\dot{m}_{desalinate}$) of the ABDCS respectively. The temperature ranges used in the study matches the practical range for a low-grade heat source long with fixed cooling water and chilled water inlet temperatures.

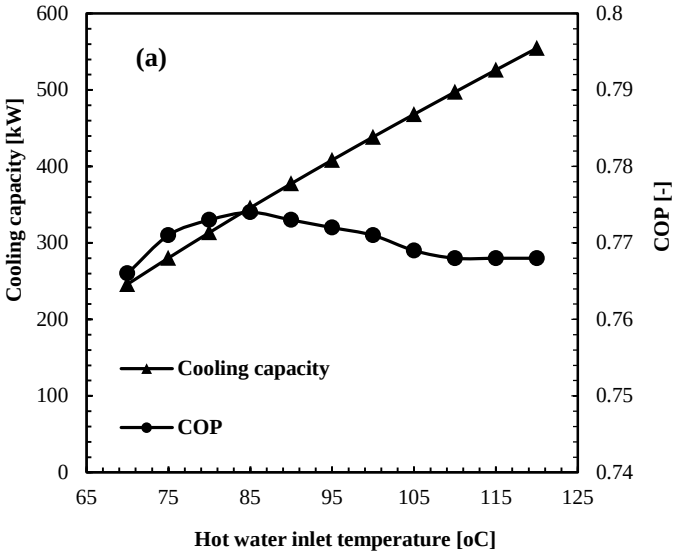

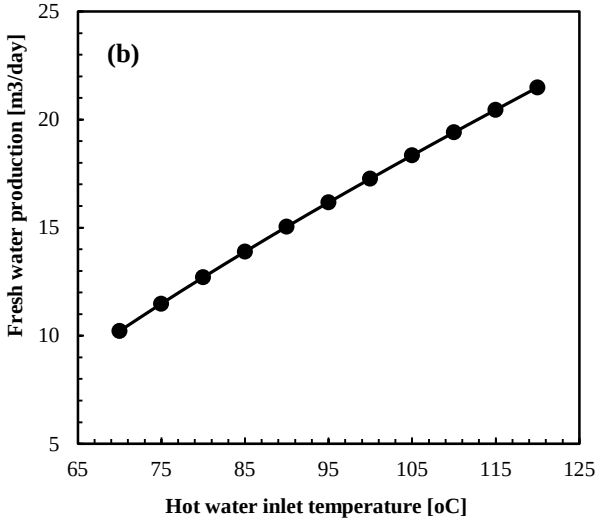

Figure 3: (a) Generator heat source temperatures with COP and cooling capacity (b) Generator heat source temperatures with desalinated water

As shown, the cooling capacity changes linearly starting from 245 kW up to 554 kW as the hot water inlet temperature increasing from 70 ^{o}C to 120 ^{o}C. This is because increasing generation temperature increases the rate of water evaporation causing further water vapor absorbed from the evaporating unit results in more cooling effect. On the other hand, the system performance (COP) is expected to rise with increasing heat source temperatures and reduce with decreasing evaporator temperature. As shown from the Figure 3(a), the system COP are relatively insensitive to changes in heat source temperatures. As the heat source temperatures increasing from 70 ^{o}C to 85 ^{o}C, the COP raises from 0.766 to 0.774. After 85 ^{o}C, increasing the heat source temperature leads to reduces in the COP gradually. This is due to increasing heat source temperatures leads to an increase in the heat losses and the irreversibility's causing the overall system performance is reduced slightly. The maximum COP value is 0.774 is obtained at 85 ^{o}C.

Figure 3(b) shows the effect of heat source temperatures (T11) on the desalinated water ($\dot{m}_{desalinate}$), while all other inputs parameters are constant. As shown, the desalinated water increases linearly from 10.22 to 21.49 m^3 per day when the heat source temperatures increase from 70 ^{o}C to 120 ^{o}C. This is because, increasing heat source temperature encourages more water vapor absorbed from the evaporator. This results in an increase in water vapor rejected from the generator to condenser and then yields more distillate water production.

Figures 4 (a and b) shows the effect of cooling water temperature on the system performance COP and cooling capacity and on the rate of desalinated water ($\dot{m}_{desalinate}$) of the ABDCS respectively.

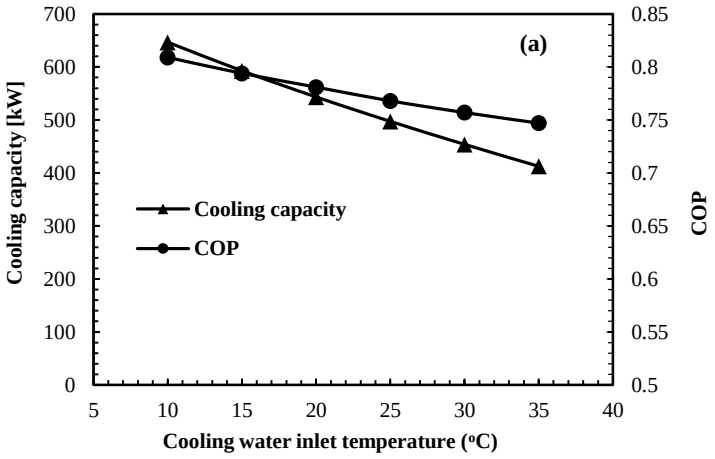

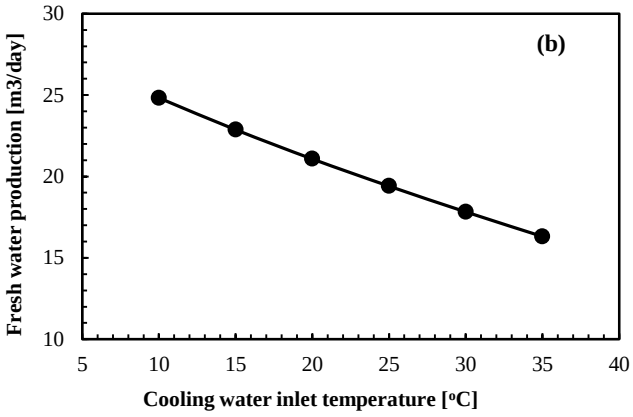

Figure 4: (a) Cooling water temperature effect on cooling capacity and COP (b) Cooling water temperature effect on freshwater production

As shown from the Figure, the cooling capacity increases steadily as the cooling water inlet temperature is lowered from 35 ^{o}C to 10 ^{o}C to 412 to 646 kW. This is since, decrease absorption

temperatures result in larger amounts of water vapor being absorbed from the evaporator. The simulated system COP also increase from 0.75 to 0.81 with lowering cooling water inlet temperature from 35 ^{o}C to 10 ^{o}C. The COP value reaches a maximum value of 0.81 ^{o}C at10 ^{o}C. The desalinated water ($\dot{m}_{desalinate}$) is also increases linearly from 16.31 to 24.82 m^3 per day as the cooling water inlet temperature decreases from 35 ^{o}C to 10 ^{o}C to, while all other inputs parameters are constant as shown in Figure 4 (b). This is because, decrease absorption temperatures result in larger amounts of water vapor absorbed from the evaporator and results in more distillate water production.

Figures 5(a and b) present the effect of chilled water temperatures on the system performance COP and cooling capacity and on the rate of desalinated water ($\dot{m}_{desalinate}$) of the ABDCS respectively with fixed hot and cooling water inlet temperatures.

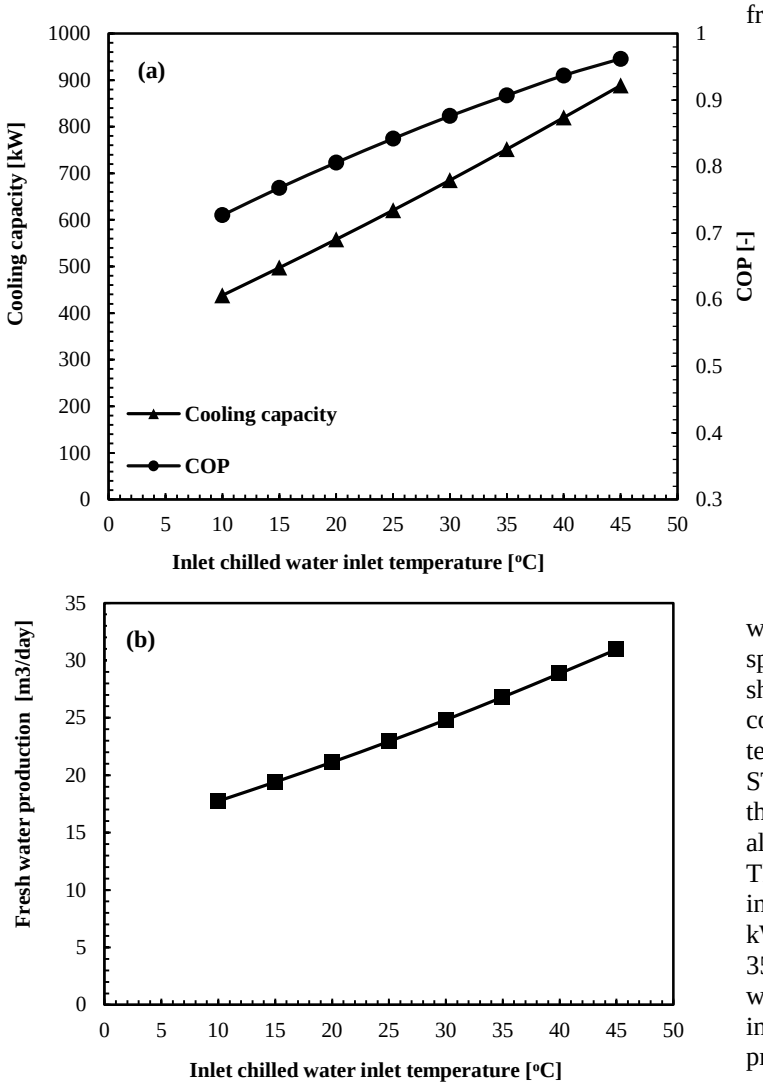

Figure 5: (a) Chilled water inlet temperatures effect on cooling capacity and COP. (b) Chilled water inlet temperature effect on freshwater production.

There is a direction for both cooling capacity and the COP to raise with the increase of the chilled water inlet temperatures, in the entire range between 10 and 45 ^{o}C. The cooling capacity raises from 438 to 888 kW over the range of inlet temperatures. As the inlet chilled water temperatures increasing, the pressure in the evaporator increases in such a way that the heat transfer driving potential increases. The COP increases also linearly from 0.73 to 0.96 over the range of chilled water temperatures from 10 and 45 ^{o}C. The evaporator inlet temperature variation causes temperature effects that balance the increased capacity in such a way that the COP increases. The sensitivity of capacity to changes in the chilled water temperature is a function of the design of the system. The desalinated water ($\dot{m}_{desalinate}$) is also enhances linearly from 17.74 to 30.95 m^3 per day as the chilled water inlet temperature increases from 10 ^{o}C to 45 ^{o}C.

Figure 6 shows the effect of system COP on the rate of freshwater production. As observed from the figure, increasing freshwater production leads to an increase in the system COP

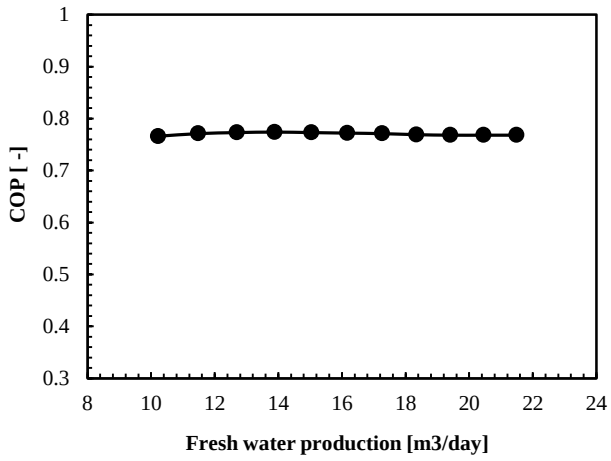

Figure 6: Relation between system COP and desalinated water.

Figure 7 shows the effect of heat source temperature, cooling water temperature, and chiller water inlet temperature on the specific thermal energy consumption (STEC). Figure 7(a and b) show the effect of raising both the hot source temperatures and cooling water temperatures on STEC. Increasing source temperatures or the cooling water temperatures increasing the STEC. The STEC for the freshwater production increases with the increase in hot source temperatures from 754 to 806 kWh/m^3 along the range of heat source temperatures from 70 to 120 ^{o}C. The STEC for the freshwater production increases with the increase in cooling water inlet temperatures from 772 to 812 kWh/m^3 along the range of cooling water temperatures from 10 to 35 ^{o}C. The STEC effect was more useful at the lowest cooling water inlet temperatures (10 ^{o}C). It was clear this because that, increasing the cooling water inlet temperatures reduced the production rates.

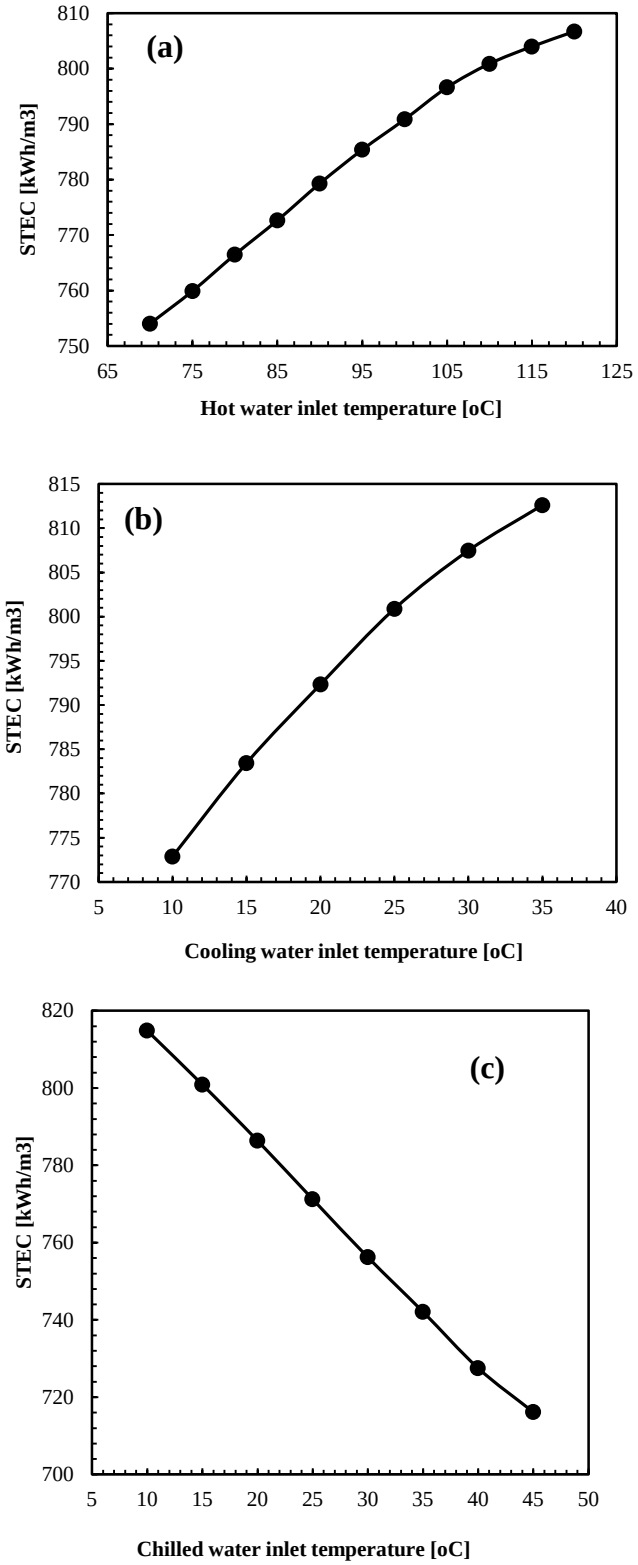

Figure 7: Effect of (a) heat source temperature, (b) cooling water temperature, and (c) chiller water inlet temperature on total specific thermal energy consumption.

Figure 7(c) shows that, the STEC decreased linearly from 814 to 716 kWh/m^3 with increasing chilled water inlet temperature from 10 to 45 ^{o}C. The STEC values drop as the chilled water inlet temperature increases. The STEC at a chilled water temperature of 45 ^{o}C reaches minimum values of 716 kWh/m^3. This is because that, the production rate increasing with increases the chilled water inlet temperatures.

5. Conclusions

This paper investigates theoretically the performance of a proposed hybrid absorption-desalination cooling system (ABDCS). The main advantage of the proposed system is its ability to utilize effectively low-grade heat source to produce simultaneously both desalinated water and cooling effect.

Results showed that, the cooling capacity increasing linearly from 245 kW up to 554 kW as the hot water inlet temperature increases from 70 ^{o}C to 120 ^{o}C. On the other hand, the system performance (COP) is also increasing with the rise in heat source temperatures. The maximum COP value 0.774 is obtained at 85 ^{o}C. The desalinated water is also increases from 10.22 to 21.49 m^3 per day when the heat source temperatures increase from 70 ^{o}C to 120 ^{o}C. This is because increasing generation temperature increases the rate of water evaporation causing further water vapor absorbed from the evaporating unit results in more cooling effect.

The cooling capacity increases steadily from 412 to 646 kW and system COP increase from 0.75 to 0.81 with lowering cooling water inlet temperature from 35 ^{o}C to 10 ^{o}C. The desalinated water ($\dot{m}_{desalinate}$) is also increases linearly from 16.31 to 24.82 m^3 per day as the cooling water inlet temperature decreases from 35 ^{o}C to 10 ^{o}C. This is since, decrease absorption temperatures result in larger amounts of water vapor being absorbed from the evaporator.

Both cooling capacity (438 to 888 kW) and the COP (0.73 to 0.96) raised with the increase of the chilled water inlet temperatures, in the entire range between 10 and 45 ^{o}C. The desalinated water is also enhanced linearly from 17.74 to 30.95 m^3 per day as the chilled water inlet temperature. The evaporator inlet temperature variation causes temperature effects that balance the increased capacity in such a way that the COP increases.

Increasing heat source temperatures or the cooling water temperatures increasing the STEC. The STEC decreased linearly from 814 to 716 kWh/m^3 with increasing chilled water inlet temperature from 10 to 45 ^{o}C.

References

[1] Harby, K., Fahad, A., 2019. An investigation of energy savings in a split air-conditioner using commercial cooling pads with different thicknesses and wide range of climatic conditions. Energy 182, 321-336.

[2] Harby, K., 2017. Hydrocarbons and their mixtures as alternatives to environmental unfriendly halogenated refrigerants: an updated overview. Renew. Sustain. Energy Rev. 73, 1247-1264.

[3] Ali, E.S., Harby, K. Askalany, A.A., Diab, M.R., Alsaman, A.S., 2017. Weather effect on a solar powered hybrid adsorption desalination- cooling system: a case study of Egypt's climate. Appl. Therm. Eng. 124, 663-672.

[4] Ehab S.A., Ahmed A.A., Harby K., Mohamed R.D., Ahmed S.A., 2018. Adsorption desalination-cooling system employing copper sulfate and driven by low grade heat sources. Appl. Therm. Eng. 136,169-176.

[5] Kabeel A.E., Mohamed A., Harby K., Amr E., 2020. Augmentation of diurnal and nocturnal distillate of modified tubular solar still having copper tubes filled with PCM in the basin. Journal of Energy Storage. 32, 101992.

[6] Kalogirou S., 1997, Economic analysis of a solar assisted desalination system. Renewable Energy. 4, 351-367.

[7] Kabeel A.E., Harby K., Mohamed A., Amr E., 2021. Performance improvement of a tubular solar still using V-corrugated absorber with wick materials: Numerical and experimental investigations. Solar energy. 217, 187-199.

[8] Kabeel A.E., Mohamed A., Harby K., Amr E., 2020. Augmentation of diurnal and nocturnal distillate of modified tubular solar still having copper tubes filled with PCM in the basin, Journal of Energy Storage. 32, 101992.

[9] Mohamed A., Harby K., Amr E., 2021. Performance improvement of modified tubular solar still by employing vertical and inclined pin fins and external condenser: An experimental study. Environmental Science and Pollution Research. 28, 13504-13514.

[10] Harby K., Ehab S. Almohammadi A., 2021. A novel combined reverse osmosis and hybrid absorption desalination-cooling system to increase overall water recovery and energy efficiency, Journal of Cleaner Production, Journal of cleaner production, 287, 125014,

[11] Alarcon, P., D.C., García-Rodríguez, L., 2007. Application of absorption heat pumps to multi-effect distillation: a case study of solar desalination. Desalination 212, 294-302.

[12] Alelyani, S.M., Fette, N.W., Stechel, E.B., Doron, P., Phelan, P.E., 2017. Techno-economic analysis of combined ammonia-water absorption refrigeration and desalination. Energy Convers. Manag. 143, 493-504.

[13] Rosiek S., 2019. Exergy analysis of a solar-assisted air-conditioning system: Case study in southern Spain. 148, 806-816.

[14] Bellos, E., Tzivanidis, C., Antonopoulos, K.A., 2016. Exergetic, energetic and financial evaluation of a solar driven absorption cooling system with various collector types. Appl. Therm. Eng. 102, 749-759.

[15] Li, M., Xu, C., Hassanien, R.H., Xu, Y., Zhuang, B. 2016. Experimental investigation on the performance of a solar powered lithium bromide-water absorption cooling system. Int. J. Refrig. 71, 46-59.

[16] García, J.R., García, F.V., Izquierdo, J.M., Marín, J.P., Martínez R.S., 2011. Modelling an absorption system assisted by solar energy. Appl. Therm. Eng. 31, 112-118.

[17] Tsilingiris, P.T., 1993. Theoretical modelling of a solar air conditioning system for domestic applications. Energy Convers. Manag., 34, 523-531.

[18] Mazloumi, M., Naghashzadegan, M., Javaherdeh, K., 2008. Simulation of solar lithium bromide-water absorption cooling system with parabolic trough collector. Energy Convers. Manag., 49, 2820-2832.

[19] Yeung M.R., Yueu P.K., Dunn A., Cornish L.S., 1992. Performance of a solar powered air conditioning system in Hong Kong. Solar energy. 48, 309-319.

[20] Altaee, A., 2012. Computational model for estimating reverse osmosis system design and performance: part-one binary feed solution. Desalination. 291, 101-105.

[21] El-Dessouky, T., Ettouney, M., 2002. Fundamentals of saltwater desalination, Chapter 7 Reverse Osmosis. first. Elsevier

[22] Li Z., Sumathy K., 2001. Simulation of a solar absorption air conditioning system. Energy Convers. Manage. 42, 313-327.

[23] ANSI/ASHRAE Standard 93-2003, Methods of Testing to Determine the Thermal Performance of Solar Collectors, ISSN 1041-2336, ASHRAE, Inc., 2003, 1791 Tullie Circle, Ne, Atlanta, GA30329.

[24] Balghouthi, M., Chahbani, M.H., Guizani, A., 2008. Feasibility of solar absorption air conditioning inTunisia. Build. Environ. 43, 1459-1470.

Nomenclature

A	Area, m^2
h	Enthalpy, $kjkg^{-1}$
$\dot{m}$	Mass flow rate, kgs^{-1}

Subscripts

abs	Absorber
b	Brine
STEC	Specific thermal energy consumption
con	Condenser
Evap	Evaporator
abs	Absorber
gen	Generator
hex	Heat exchanger
Cap	Capacity